Science Translational Medicine
AAAS

www.sciencetranslationalmedicine.org/cgi/content/full/9/385/eaak9679/DC1

Supplementary Materials for

Combined antiangiogenic and anti–PD-L1 therapy stimulates tumor immunity through HEV formation

Elizabeth Allen, Arnaud Jabouille, Lee B. Rivera, Inge Lodewijckx, Rindert Missiaen, Veronica Steri, Kevin Feyen, Jaime Tawney, Douglas Hanahan, Iacovos P. Michael, Gabriele Bergers*

*Corresponding author. Email: gabriele.bergers@kuleuven.vib.be

Published 12 April 2017, *Sci. Transl. Med.* **9**, eaak9679 (2017)
DOI: 10.1126/scitranslmed.aak9679

The PDF file includes:

Other Supplementary Material for this manuscript includes the following:
(available at www.sciencetranslationalmedicine.org/cgi/content/full/9/385/eaak9679/DC1)

Movie S1 (.avi format). HEVs with T cells in D + P + Ag–treated mice.
Movie S2 (.avi format). HEVs without T cells 1 in D + P + Ag–treated mice.
Movie S3 (.avi format). HEVs without T cells 2 in D + P + Ag–treated mice.

Materials and Methods

Animal studies

C57BL/6 Rip1-Tag2 mice were treated beginning at 13 weeks of age for two weeks (response phase) or four weeks (relapse phase) with 40 mg/kg DC101 and/or 10 mg/kg anti-PD-L1. For triple combination cohorts, LTβR agonist or antagonist was dosed at 2 mg/kg the day after DC101 + anti-PD-L1. All drugs were injected intraperitoneally (i.p.) twice a week. For tumor burden analysis of Rip1-Tag2 mice (Fig 3A), the following numbers of mice were used: control IgG two weeks (13-15W) n=8, DC101 two weeks (13-15W) n=8, anti-PD-L1 2W (13-15W) n=8, combination DC101 + anti-PD-L1 two weeks (13-15W) n=11, DC101 four weeks (13-17W) n=11, combination DC101 + anti-PD-L1 four weeks (13-17W) n=11. Tumor burden measurement for each Rip1-Tag2 mouse was equal to the sum of individual tumors per mouse.

Orthotopic breast cancer experiments were performed using a cell line generated from FVB MMTV-PyMT mammary tumors (Zena Werb, UCSF). 100,000 PyMT cells were implanted into the 4th mammary fat pad of FVB/n female mice, then allowed to establish until they reached approximately 5 mm in diameter. Mice were then dosed with single, double, or triple combinations of DC101, anti-PD-L1, and LTβR agonist or antagonist as described in the preceding paragraph. For tumor burden analysis of MMTV-PyMT tumor-bearing mice, 15 mice were used for each group (IgG two weeks, DC101 two weeks, anti-PD-L1 two weeks, combination of DC101 + anti-PD-L1 two weeks, Fig. 3A). For survival trials, 4 mice per cohort were used (Fig. 7G).

Orthotopic glioblastoma experiments were performed using the cell line NFpp10 generated from embryonic C57/Bl6 neural stem cells infected with shP53-shNF1 and shPTEN-containing lentiviral vectors (Inder Verma, Salk Institute) (*68*). $2x10^5$ NFpp10-GBM cells were implanted into the striatum (x=0.1 mm; y=2 mm on the right; z=3 mm) of C57BL/6

females and males. Nine days later, mice were dosed with single drugs and combination of 15 mg/kg B20S and 10 mg/kg anti-PD-L1 twice a week by i.p. injection over two weeks. For experiments assessing the HEV formation through the activation of the LTβR signaling, 2 mg/kg of anti-LTβR antibody was administered twice weekly in combination with B20S and anti-PD-L1 over two weeks. Tumor burden of NFpp10-GBM-bearing mice was defined by excising and measuring the GFP^+ tumor from the brain under a binocular fluorescent microscope. 4 mice were used for each group (IgG two weeks, anti-LTβR two weeks, combination + anti-PDL1 two weeks, and combination B20S + anti-PD-L1 + anti- LTβR two weeks).

Tumor burden for all tumor models was calculated using the following formula to approximate the volume of an ellipsoid: $0.52x(width)^2x(length)$.

B20S production

Anti-mouse and human VEGF B20 biosimilar (B20S) was generated based on the previously published sequence of B20-4.1 (*69*). The variable regions of the heavy and light chain of B20-4.1 were fused to the constant region of IgG1 and κ chain, respectively. Stable mammalian 293 cell lines for recombinant B20S production were established using the piggyBac transposon system (*70*). Briefly, the two genes coding for the heavy and light chain were cloned into two different PB-T-RfA transposons. Recombinant B20S was purified using a Protein A affinity column and stored in 50 mM sodium phosphate buffer containing 150 mM NaCl (pH 7.0).

Gene expression analysis

qPCR expression analyses were performed with the indicated primer sets (table S1) on cell lines in vitro or FACS-sorted tumor cell populations ex vivo. For ex vivo studies, pre-amplified cDNA from sorted cells was made using the Cells Direct kit (Invitrogen, #11754100) according to the manufacturer's protocol. qPCR was then performed on an AB7900HT instrument (Applied Biosystems) by using the pre-amplified cDNA for the target genes. qPCR analysis was performed using Power-Up SYBR green mastermix (Thermo Scientific, #A25742). Relative gene expression was calculated as previously described (*71*). In brief, *Rpl19* or *Gapdh* were used as housekeeping genes to generate ΔCt. ΔCt values from untreated mice were used as reference for the treatment groups to generate ΔΔCt, and relative gene expression was calculated as $2^{(-\Delta\Delta Ct)}$, or presented as copy number/1,000 copies of *Gapdh* to calculate gene expression. Analyses of sorted cells from tumor-bearing mice were performed using at least two independent experiments and a minimum of 3 to 5 experimental mouse replicates for each treatment condition. All reactions were run in duplicate. For primer sequences, see table S1.

FACS

Brefeldin A (Ebioscience, #00-4506-51) was intraperitoneally injected into tumor-bearing mice six hours before tumor harvest to enable flow cytometric detection of T cells and intracellular cytokines **(*72*)**. Tumors were then harvested from PBS-perfused mice and processed as previously described **(*17*)**. Cells were treated with Fc-block and stained with allophycocyanine (APC)-conjugated anti-CD3 (clone 17A2, BioLegend, #100235), brilliant violet 510-conjugated anti-CD4 (clone RM4-5, BioLegend, #100533), evolve 655-conjugated anti-CD8 (clone 53-6.7, eBioscience, #86-0081-41), phycoerythrin (PE)-conjugated anti-

Granzyme B (clone NGZB, eBioscience, #12-8898-82), peridinin chlorophyll-Cy5.5 (PerCP-Cy5.5)-conjugated anti-interferon-γ (clone XMG1.2, eBioscience, 47-7311-80), PE-conjugated anti-PD-L1 (clone 10F.9G2, Molecular Probes, #A18683), PerCP-Cy5.5-conjugated anti-CD45 (clone 30F-11, eBioscience, 45-0451-80), efluor 450-conjugated anti-CD11c (clone N418, eBioscience, #48-0114-80), APC-conjugated anti-CD31 (clone 390, eBioscience, #17-0311-80), brilliant violet 510-conjugated anti-CD11b (BioLegend, #101245), fluorescein isothiocyanate (FITC)-conjugated anti-insulin (CST, #9016S), FITC-conjugated anti-EpCAM (clone G8.8, eBioscience, #11-5791-80). CTLs were sorted as $CD3^+CD8^+$ cells. Tumor cells were sorted as $CD45^-insulin^+$ cells from tumors of RT2-PNET mice, $CD45^-EpCAM^+$ cells from tumors of MMTV-PyMT mice, and $CD45^-GFP^+$ cells from tumors of NFpp10-GBM mice. Endothelial cells were identified as $CD45^-CD31^+$ cells, and myeloid cells were recognized as $CD45^+CD11b^+$ cells. Dendritic cells were isolated as $CD45^+CD11c^+$ and $CD11b^+CD11c^+$ cells. Compensation was performed using singly-stained beads (BD Biosciences, #560499). Data were analyzed using FlowJo software (Treestar). Analyses of sorted cells from tumor-bearing mice were performed using at least two independent experiments and a minimum of 3 to 5 experimental mouse replicates for each treatment condition.

Immunostaining

Immunohistochemistry and Immunofluorescence were conducted on frozen tissue sections. To prepare frozen tissue, excised pancreata or tumors were fixed in 2-4% paraformaldehyde at 4°C overnight followed by 30% sucrose at 4°C overnight before being embedded in OCT (Tissue Tek). Tumor tissue sections were stained with Alexa Fluor (AF) 488-conjugated anti-MECA79 (eBioscience, #53-6036-82), APC-conjugated anti-CD45 (clone 30-F11, eBioscience, #17-045-1-82), FITC-conjugated anti-CD31 (clone MEC13.3, BD Pharmingen,

#553372), APC-conjugated anti-CD31 (clone 390, eBioscience, #17-0311-80), PE-conjugated anti-PD-L1 (clone 10F.9G2, Molecular probes, #A18683), PE-conjugated CD11c (clone N418, eBioscience, #12-0114-82), AF 647-conjugated anti-CD4 (clone RM4-5, BioLegend, #100530), APC-conjugated anti-CD3 (clone 17A2, BioLegend, #100236), APC-conjugated anti-CD8 (clone 53-6.7, eBioscience, #100711), FITC-conjugated anti-B220 (clone RA3-6B2, ebioscience, #11-0452-82), biotinylated anti-Granzyme B (R&D Systems, #BAF1865) anti-CD31 (Millipore, #MAB1398Z), anti-CD31 (Abcam, #28364), anti-phospho-S6 (CST, #4858), anti-CA9 (Novus Biologicals, #NB100-417), and anti-cleaved caspase 3 (CST, #9664). When primary antibodies were unlabeled, fluorophore-conjugated secondary antibodies were used. Images were taken with an Observer Z1 microscope (Zeiss) linked to an AxioCam MRM camera (Zeiss) with objectives of 20x or 40x magnification. Image analysis and quantitation were performed using NIH ImageJ software on 3 representative images per mouse from at least 3 mice per group from each tumor model.

Evaluation of necrosis

Frozen tissue sections of tumors were histochemically stained with hematoxylin-eosin (H&E). H&E sections were subsequently imaged under fluorescence conditions (488 nm), using a LeicaDM5500 fluorescent microscope (10x magnification), allowing for identification of necrotic regions through autofluorescent properties of necrotic cells (*73*). Necrosis was quantified by measuring the fluorescent areas and normalized to the total tumor area using NIH ImageJ software.

Cell death and proliferation

Cell death of cultured tumor cells from RT2-PNET (β-TC3), MMTV-PyMT, and NFpp10-engineered GBM treated with LTβR agonist or antagonist was assessed using the Bioluminescence Cytotoxicity Assay Kit (BioVision, # K312-500), and proliferation was analyzed using the MTS Cell Proliferation Colometric Assay Kit (Biovision, #K300-500) according to the manufacturer's instructions; 22 mM H_2O_2 treatment was a positive control for the cytotoxicity assay. Analyses were performed using 6 replicates for each treatment condition.

Cell culture and RNA extraction

Bone marrow-derived cells (BDMCs) were isolated from C57B/L6 long bones (femurs and tibiae) of adult mice and cultured in complete RPMI medium supplemented with 20 ng/ml Granulocyte-macrophage colony-stimulating factor (GM-CSF). Non-adherent cells were removed at day 2, and fresh medium with 20 ng/ml GM-CSF was added for culturing attached BMDCs. β-TC3 RT2-PNET and MMTV-PyMT cells were cultured in DMEM high glucose supplemented with sodium pyruvate, non-essential amino acids, glutamine, and 10% FBS. NFpp10-GBM cells were cultured in DMEM: Ham's F12 medium supplemented with N-2 (Gibco), 50 μg/ml of heparin, and 20 ng/ml each of bFGF and EGF. HcMEC/D3 were cultured in complete EBM-2 medium (Lonza). Cells were plated on 48-well plates and treated for the indicated amounts of time as follows: B20S (50 μg/ml), IFNγ (50 ng/ml), or 1% O_2 (hypoxia). Cells were then washed with cold PBS, and RNA extraction was performed with TRIzol (Invitrogen).

Supplementary Figures:

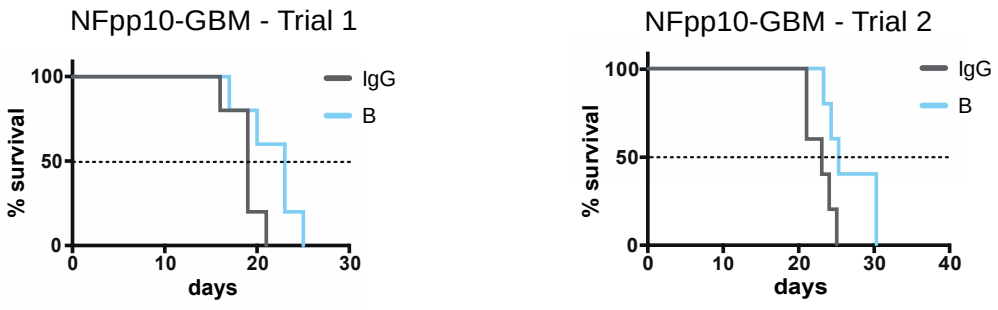

Fig. S1. Anti-VEGF therapy (B20S) does not prolong survival of NFpp10-GBM–bearing mice. Survival of NFpp10-GBM-bearing mice treated with either IgG or B (B20S). For all panels: IgG, n=4-5; B, n=5. Dotted line indicates 50% survival. Trial 1, p=0.1064 *vs* IgG; Trial 2, p=0.0858 *vs* IgG; Log-rank test for survival.

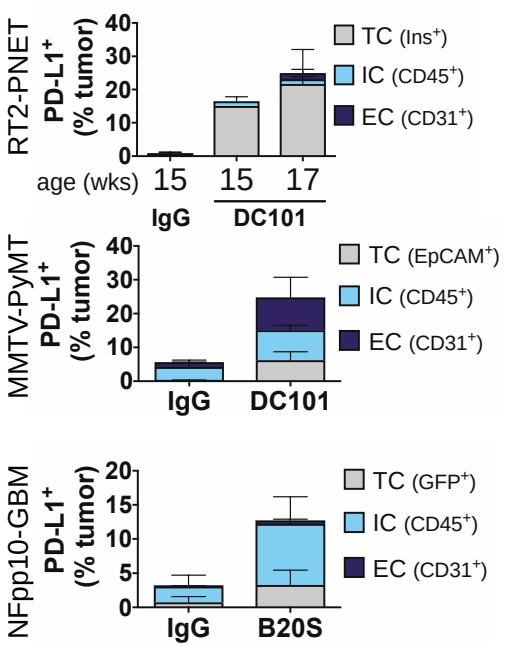

Fig. S2. PD-L1 up-regulation during antiangiogenic therapy correlates with tumor relapse. Quantitation of PD-L1^{+} tumor cells, endothelial cells (CD31^{+}), and immune cells (CD45^{+}) by immunofluorescent staining in tumor sections from RT2-PNET, MMTV-PyMT,

and NFpp10-GBM mice treated with IgG, DC101, or B20S. Data are represented as mean ± SEM. RT2-PNET: DC101 15W (n=5) *vs* IgG 15W (n=8), p=0.0041 for TC, p=0.0452 for IC, p=0.237 for EC; DC101 17W (n=7) *vs* IgG 15W, p=0.0014 for TC, p=0.0023 for IC, p=0.0121 for EC. MMTV-PyMT: DC101 (n=7) *vs* IgG (n=5), p=0.0025 for TC, p=0.0424 for IC, p=0.0159 for EC. NFpp10-GBM: B20S (n=6) *vs* IgG (n=7), p=0.0140 for TC, p=0.0012 for IC, p=0.1 for EC. Statistical analysis by Mann-Whitney test**.**

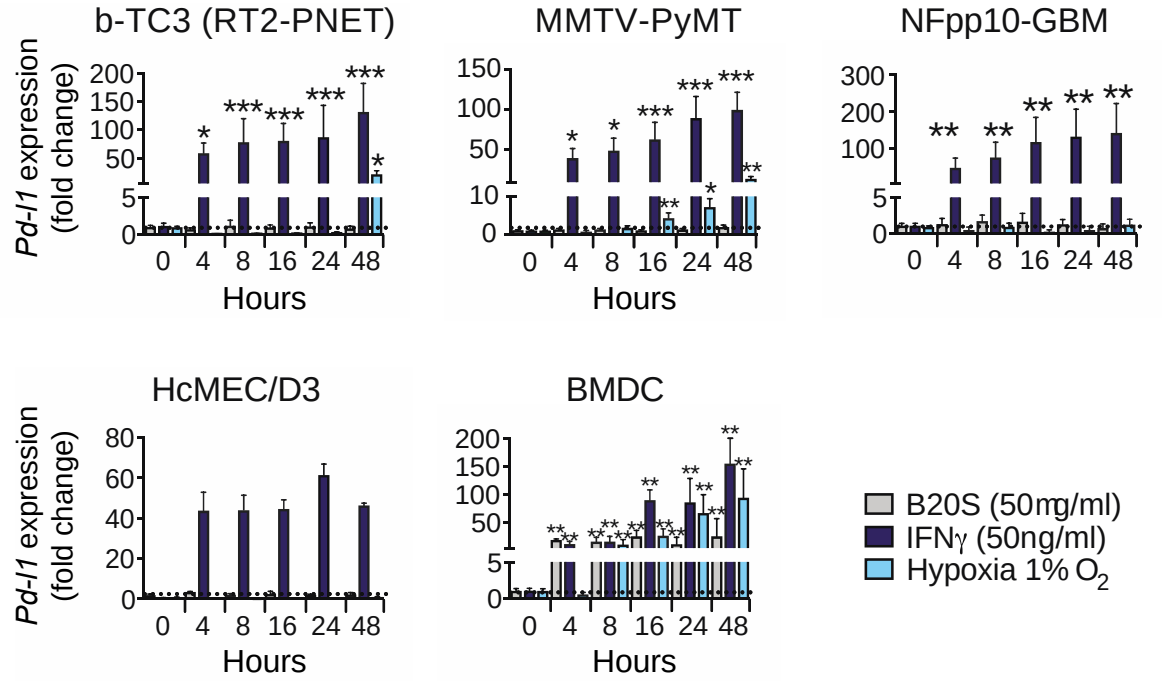

Fig. S3. IFNγ induces PD-L1 expression in several cell types. qPCR-based assessment of PD-L1 expression in tumor cells from RT2-PNET (β-TC3) and MMTV-PyMT mice as well as NFpp10-engineered GBM cells, human microvascular endothelial cells (HcMEC/D3), and murine bone marrow-derived cells (BMDCs), treated for different amounts of time with either B20S or interferon-γ (IFNγ), or incubated with 1% O_2. Dotted line indicates baseline gene expression in untreated samples. Data are represented as mean ± SEM. *p<0.05; **p<0.01; ***p<0.001; Mann-Whitney test. Black asterisks represent p-values for comparisons between untreated conditions and different time points for the same treatment.

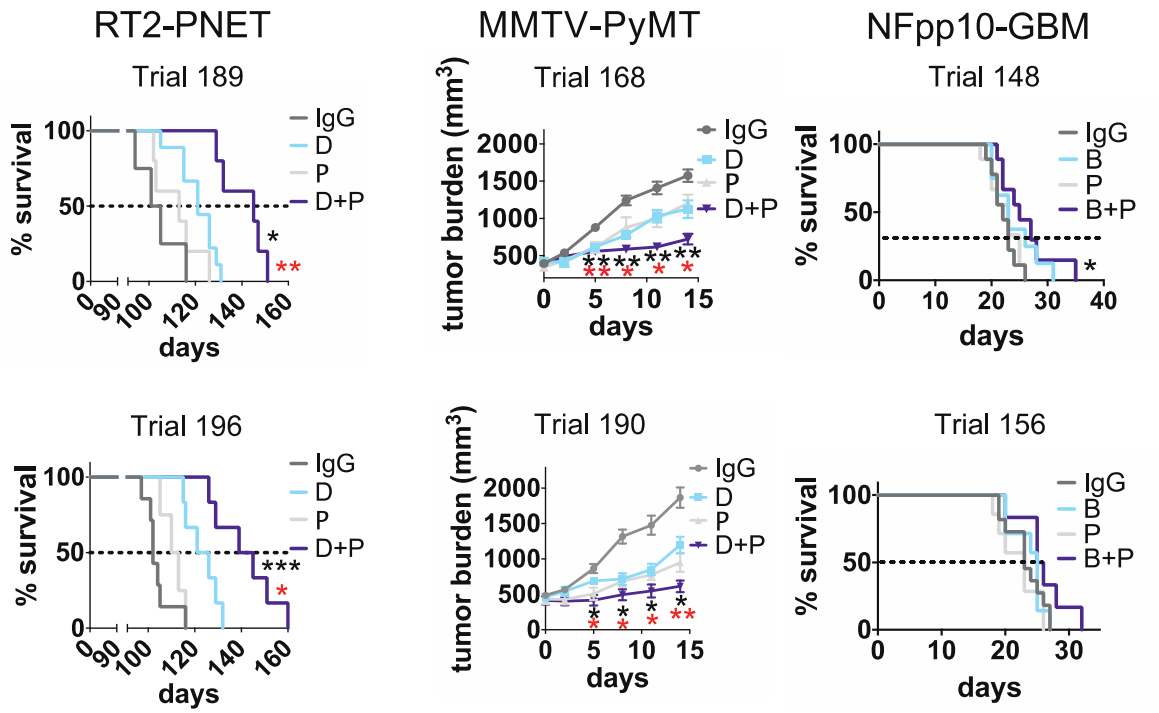

Fig. S4. Anti–PD-L1 treatment improves the effectiveness of antiangiogenic therapy in RT2-PNET and MMTV-PyMT, but not NFpp10-GBM. Survival or tumor burden analyses in RT2-PNET, MMTV-PyMT, and NFpp10-GBM mice under different treatment conditions. IgG (RT2-PNET: trial 189, n=4; trial 196, n=7; MMTV-PyMT: trial 168, n=6; trial 190, n=4; NFpp10-GBM: trial 148, n=9; trial 156, n=11), DC101 (RT2-PNET: trial 186, n=5; trial 196, n=6; MMTV-PyMT: trial 168, n=6; trial 190, n=5), or B20S (NFpp10-GBM: trial 148, n=8; trial 156, n=7), anti-PD-L1 (RT2-PNET: trial 189, n=5; trial 196, n=4; MMTV-PyMT: trial 168, n=6; trial 190, n=5; NFpp10-GBM: trial 148, n=9; trial 156, n=7), or combination therapy (RT2-PNET: trial 189, n=5: trial 196, n=6; MMTV-PyMT: trial 168, n=6; trial 190, n=5; NFpp10-GBM: trial 148, n=9; trial 156, n=6). Dotted line indicates 50% survival. Data are represented as mean ± SEM for tumor burden. *p<0.05; *p<0.01; ***p<0.001; Mann-Whitney test or Log-rank test for survival. Black asterisks represent p-values for comparisons between IgG and different treatments; red asterisks represent p-values for other comparisons. D=DC101; P=anti-PD-L1; B=B20S.

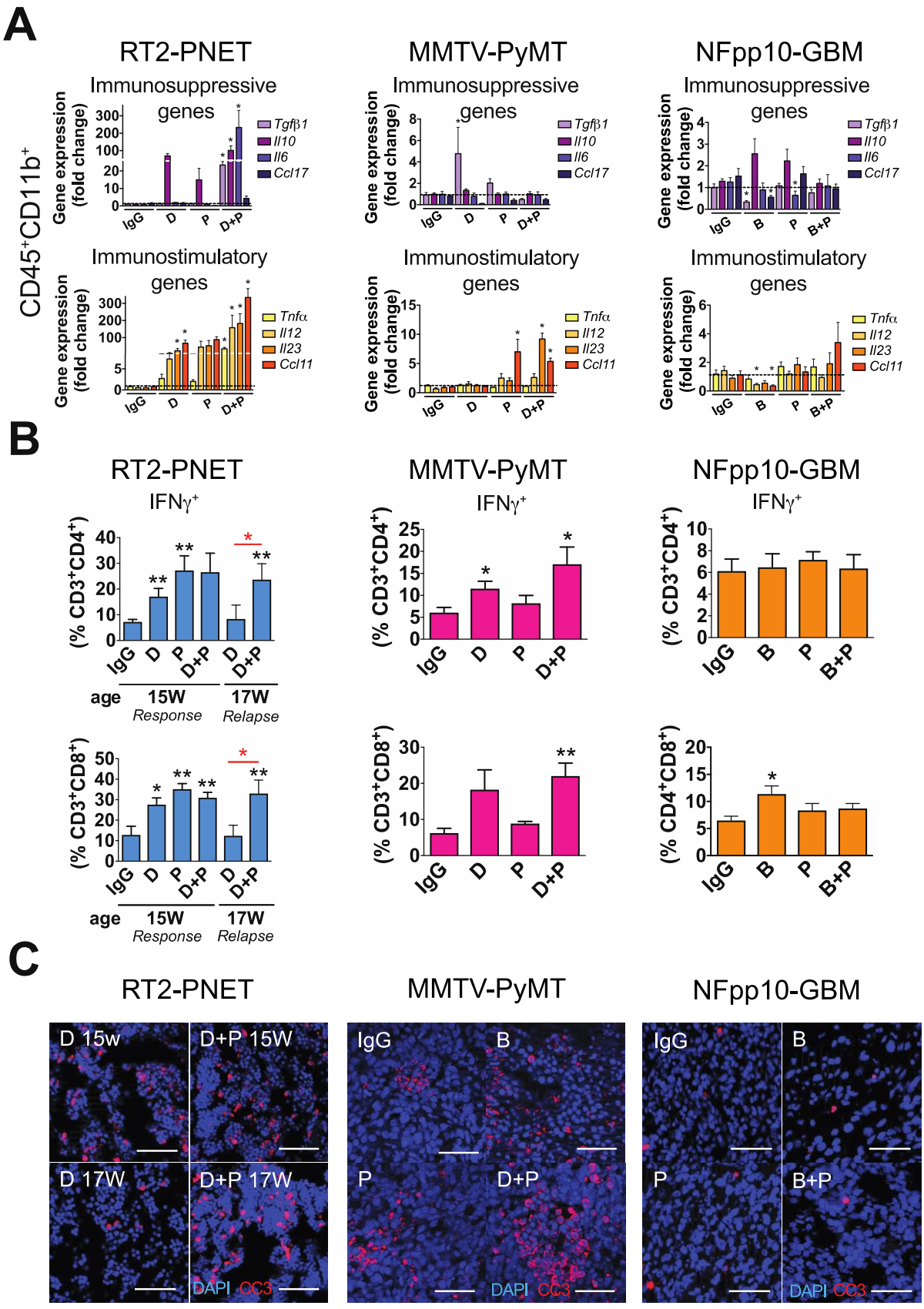
A
RT2-PNET
MMTV-PyMT
NFpp10-GBM
CD45+CD11b+
Immunosuppressive genes
Immunostimulatory genes
Gene expression (fold change)
Tgfβ1
Il10
Il6
Ccl17
Tnfα
Il12
Il23
Ccl11
IgG
D
P
D+P
B
B+P
B
RT2-PNET
MMTV-PyMT
NFpp10-GBM
IFNγ+
(% CD3+CD4+)
(% CD3+CD8+)
(% CD4+CD8+)
age
15W
17W
Response
Relapse
C
RT2-PNET
MMTV-PyMT
NFpp10-GBM
D 15w
D+P 15W
D 17W
D+P 17W
IgG
B
P
D+P
B+P
DAPI
CC3

Fig. S5. Antiangiogenic + anti–PD-L1 treatment correlates with an immunostimulatory microenvironment and enhanced apoptosis in responsive tumors. (**A**) qPCR-based expression analyses of immunostimulatory and immunosuppressive genes in $CD45^+CD11b^+$ cells from RT2-PNET mice treated for 4 weeks, or MMTV-PyMT and NFpp10-GBM mice treated for 2 weeks. (**B**) FACS analysis of $IFN\gamma^+CD3^+CD4^+$ and $IFN\gamma^+CD3^+CD8^+$ T cells in RT2-PNET (IgG, n=6/6; D/15W, n=6/6; P, n=6/6; D+P/15W, n=7/6; D/17W, n=3/3; D+P/17W, n=6/5), MMTV-PyMT (IgG, n=6/5; D, n=6/6; P, n=7/4; D+P, n=6/6), and NFpp10-GBM (IgG, D, P, D+P, n=6/7). (**C**) Representative images of $CC3^+$ cells in RT2-PNET, MMTV-PyMT, and NFpp10-GBM tumors. Scale bars, 50 μm. Dotted line indicates baseline gene expression in IgG-treated samples. Data are represented as mean ± SEM. *p<0.05; **p<0.01; Mann-Whitney test. Black asterisks represent p-values for comparisons between IgG and different treatments; red asterisks represent p-values for other comparisons. D=DC101; P=anti-PD-L1; B=B20S; IFNγ=interferon-γ; CC3=cleaved caspase 3.

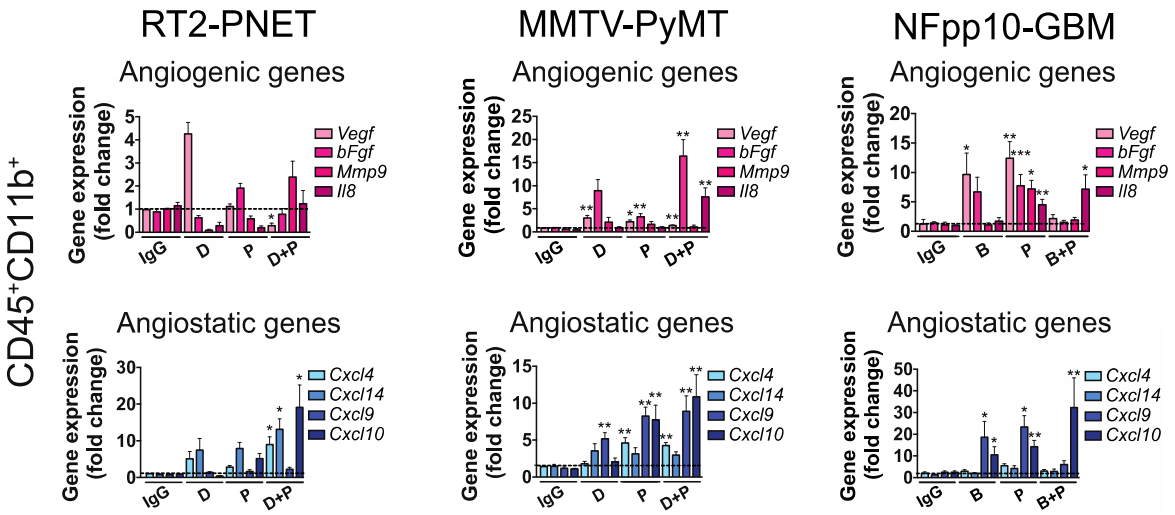

Fig. S6. Antiangiogenic + anti–PD-L1 treatment increases angiostatic activity of intratumoral myeloid cells in responsive tumors. qPCR-based expression analyses of angiogenic and angiostatic genes in $CD45^{+}CD11b^{+}$ cells from RT2-PNET, MMTV-PyMT, and NFpp10-GBM tumors after 2 weeks of treatment. Dotted line indicates baseline gene expression in IgG-treated samples. Data are represented as mean ± SEM. *p<0.05; **p<0.01; ***p<0.001; Mann-Whitney test. Black asterisks represent p-values for comparisons between IgG and different treatments. D=DC101; P=anti-PD-L1; B=B20S.

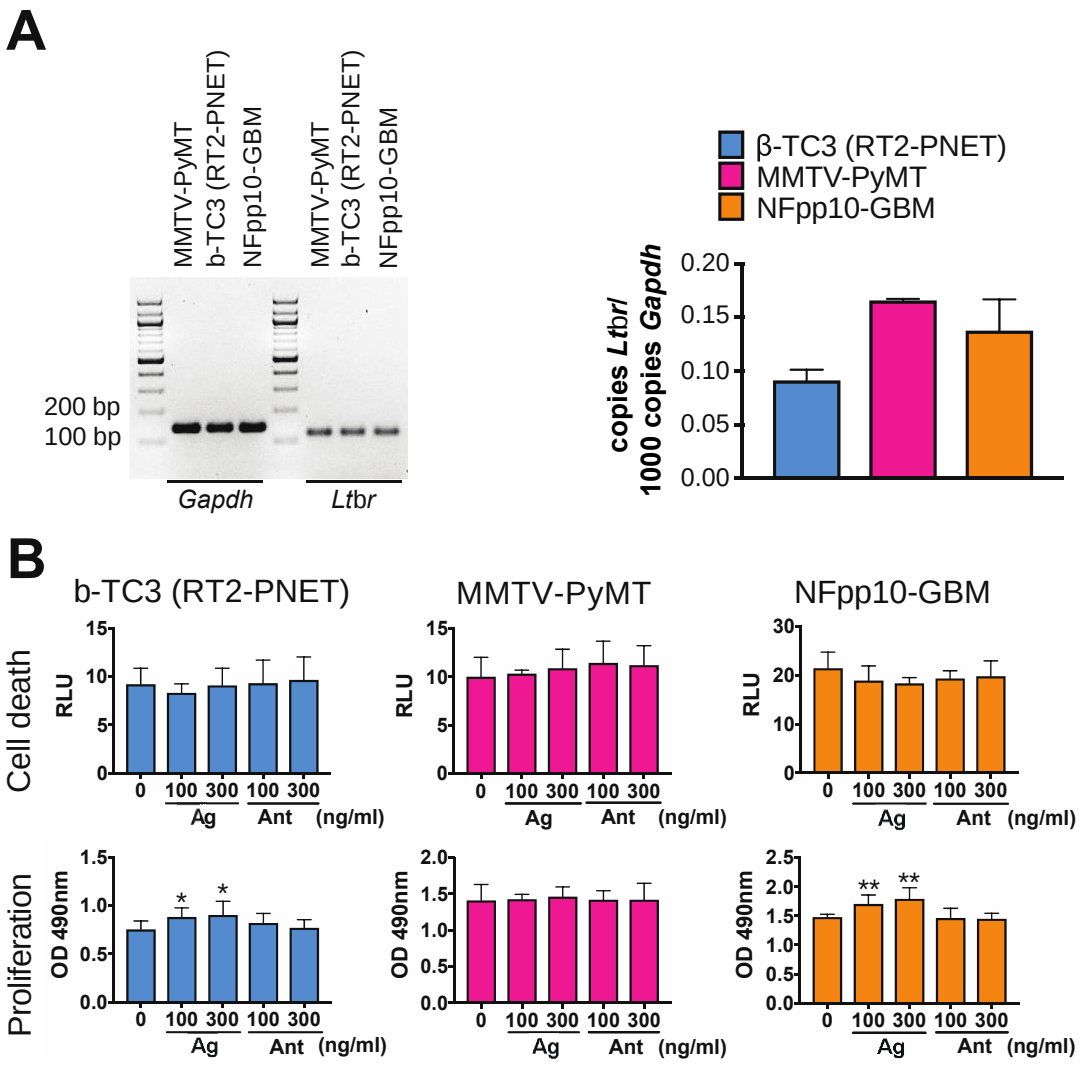

Fig. S7. LTβR agonist and LTβR antagonist do not affect TC proliferation or death. (**A**) qPCR-based expression analysis for *Ltβr* expression in tumor cell lines was performed in triplicate using *Gapdh* as a control. Products were run on an agarose gel. *Ltβr* expression relative to *Gapdh* for β-TC3 (RT2-PNET), MMTV-PyMT, and NFpp10-GBM cell lines. (**B**) Cell death/cytotoxicity was assessed using the Bioluminescence Cytotoxicity Assay kit, and proliferation was analyzed using the MTS Cell Proliferation Colorimetric Assay kit at 48 hours after treatment with the LTβR agonist and antagonist. Data are represented as mean ± SEM. *p<0.05; **p<0.01; Mann-Whitney. Black asterisks represent p-values for comparisons between control and differing treatments. Ag=anti-LTβR agonist; Ant=anti-LTβR antagonist.

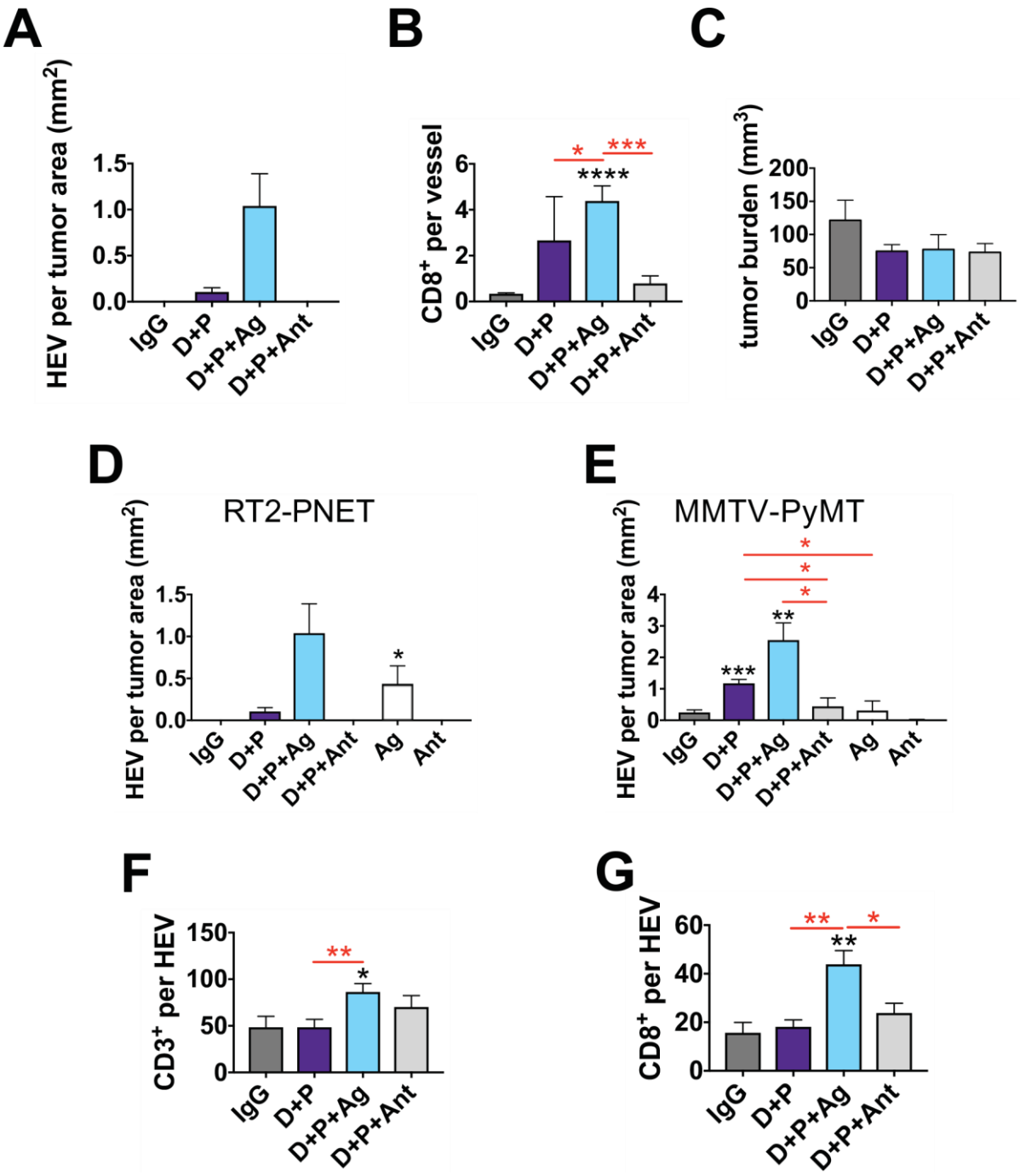

Fig. S8. LTβR agonist enhances and LTβR antagonist decreases HEVs and T cell influx in RT2-PNET and PyMT tumors. (**A**) Number of HEVs/mm^2 tumor area. IgG, n=4; D+P, n=5; D+P+Ag, n=4; D+P+Ant, n=3. (**B**) Number of CD8$^+$ cells around tumor vessels. IgG, n=7 (0 HEVs); D+P, n=8 (1 HEV); D+P+Ag, n=41 (26 HEVs); D+P+Ant, n=8 (1 HEV). (**C**) Tumor burden of RT2-PNET mice under different treatment conditions. IgG, n=6; D+P, n=4; D+P+Ag, n=4; D+P+Ant, n=6. (**D**) Number of HEVs/mm^2 tumor area in RT2-PNET. IgG,

n=4; D+P, n=5; D+P+Ag, n=4; D+P+Ant, n=3; Ag, Ant, n=3. (**E**) Number of HEVs/mm^2 tumor area in MMTV-PyMT. IgG, D+P, n=8; D+P+Ag, D+P+Ant, n=5; Ag, Ant, n=2. (**F**) Number of CD3$^+$ cells around HEVs in RT2-PNET. IgG, n=5; D+P, n=11; D+P+Ag, n=28; D+P+Ant, n=10. (**G**) Number of CD8$^+$ cells around HEVs in MMTV-PyMT. IgG, n=5; D+P, n=11; D+P+Ag, n=28; D+P+Ant, n=10. Data are represented as mean ± SEM. *p<0.05; **p<0.01; ***p<0.001; ****p<0.0001; Mann-Whitney test. Black asterisks represent p-values for comparisons between IgG and different treatments; red asterisks represent p-values for other comparisons. D=DC101; P=anti-PD-L1; Ag=anti-LTβR agonist; Ant=anti-LTβR antagonist.

Table S1. Primers for qPCR-based expression analysis.

Species	Gene	Forward primer (5' → 3')	Reverse primer (5' → 3')
Mouse	*Gapdh*	CTTTGTCAAGCTCATTTCCTGG	TCTTGCTCAGTGTCCTTGC
	Rpl19	CTGGATGAGAAGGATGAGGATC	GGATGTGCTCCATGAGGATG
	Vegf	CAGGCTGCTGTAACGATGAA	GCATTCACATCTGCTGTGCT
	bFgf	GGCTGCTGGCTTCTAAGTGT	CCGTTTTGGATCCGAGTTTA
	Mmp9	GCCCTGGAACTCACACGACA	TTGGAAACTCACACGCCAGAAG
	Il8	TGCCCTACGGTGGAAGTCATA	TGCATTCCGCTTAGCTTTCTTT
	Cxcl4	TGCACTTAAGAGCCCTAGACCCAT	AGATCTCCATCGCTTTCTTCGGGA
	Cxcl14	GAAGATGGTTATCGTCACCACC	CGTTCCAGGCATTGTACCACT
	Cxcl9	GGAGTTCGAGGAACCCTAGTG	GGGATTTGTAGTGGATCGTGC
	Cxcl10	TCCCTCTCGCAAGGAC	TTGGCTAAACGCTTTCAT
	Tgfβ1	GCGGACTACTATGCTAAAGAGGTCAC	TTTCTCATAGATGGCGTTGTTGC
	Il10	CAGGGATCTTAGCTAACGGAAA	GCTCAGTGAATAAATAGAATGGGAAC
	Il6	GAGGATACCACTCCCAACAGACC	AAGTGCATCATCGTTGTTCATACA
	Ccl17	ACCATGAGGTCACTTCAGATGC	AATGGCCCCTTTGAAGTAATCC
	Tnfα	CGGAGTCCGGGCAGGT	GCTGGGTAGAGAATGGATGAACA
	Il12	AGTCCCTTTGGTCCAGTGTG	AGCAGTAGCAGTTCCCCTGA
	Il23	CCAGCGGGACATATGAATCT	AGGCTCCCCTTTGAAGATGT
	Ccl11	GAATCACCAACAACAGATGCAC	ATCCTGGACCCACTTCTTCTT
	Pd-l1	GACGCAGGCGTTTACTGCT	GCGGTATGGGGCATTGACTTT
	Light	GCATCAACGTCTTGGAGACA	ATACGTCAAGCCCCTCAAGA
	Il7	TTCCTCCACTGATCCTTGTTCT	AGCAGCTTCCTTTGTATCATCAC
	Ccl7	ATTATGGGTGGTGAGAGCCG	CCAGGGACACCGACTACTG
	Ccl21	GTGATGGAGGGGGTCAGGA	GGGATGGGACAGCCTAAACT
	Ccl19	ATGTGAATCACTCTGGCCCAGGAA	AAGCGGCTTTATTGGAAGCTCTGC
	Cxcl13	GGCCACGGTATTCTGGAAGC	GGGCGTAACTTGAATCCGATCTA
	Glycam1	CCACCAGCTACACCAGTGAG	CCTGGGCCTCTTGATTCTCTG
	Cd40	GCAGTGTGTTACGTGCAGTG	TGTGCAGTGGCTTGTCAGTC
	Perforin	AAAAACTCCCTAATGAGAGACGC	ACACGCCAGTCGTTATTGATATT
	Mx1	CAAAGCCCTGGAAGAGTCTG	GGGATCTGTCTCCCAATATT
	Ifit3	AGCACAGAAACAGATCACCAT	CACCCTGTCTTCCATATGACTG
	Ltβr	TGGTGCCCCCTTATCGCATA	TGCATACCGCAAAGACAAACTC
Human	*GAPDH*	AAGGTGAAGGTCGGAGTCAA	AATGAAGGGGTCATTGATGG
	PD-L1	TGGCATTTGCTGAACGCATTT	TGCAGCCAGGTCTAATTGTTTT

Table S2. Summary of experimental *P* values.

Fig 2A, B. C	% $CA9^+PD\text{-}L1^+$	$IFN\gamma^+$ % $CD3^+CD4^+$	$IFN\gamma^+$ % $CD3^+CD8^+$	% GzB^+
RT2-PNET				
IgG *vs*. DC101	0.0216	0.0022	0.026	0.026
MMTV-PyMT				
IgG *vs*. DC101	0.0089	0.026	0.0519	0.026
NFpp10-GBM				
IgG *vs*. B20S	0.0476	0.6991	0.0262	0.0152

Fig 2D	*Cxcl10*		*Mx1*		*Ifit3*	
	$PD\text{-}L1^-$ IgG *vs.* DC101	$PD\text{-}L1^+$ IgG *vs.* DC101	$PD\text{-}L1^-$ IgG *vs.* DC101	$PD\text{-}L1^+$ IgG *vs.* DC101	$PD\text{-}L1^-$ IgG *vs.* DC101	$PD\text{-}L1^+$ IgG *vs.* DC101
RT2-PNET						
TC	0.1049	0.3282	0.007	0.1304	0.1049	0.1949
EC	0.0003	0.0281	0.0002	0.0003	0.0104	0.0006
IC	0.5054	0.0047	0.5737	0.083	0.1949	0.003
MMTV-PyMT						
TC	0.0002	0.0207	0.1049	0.2786	0.0002	0.0379
EC	0.0002	0.0379	0.0002	0.1605	0.0002	0.6126
IC	0.8785	0.0047	0.0379	0.0499	0.5737	0.0003
NFpp10-GBM						
TC	0.9143	0.0095	>0.9999	0.0381	0.2571	0.0095
EC	0.9429	0.1143	0.1095	0.6429	0.2	0.8048
IC	>0.9999	>0.9999	0.1333	0.7546	0.8	0.008

Fig 3A RT2-PNET	Tumor burden
IgG *vs.* D 15W	0.0006
IgG *vs.* P 15W	0.1369
IgG *vs.* D+P 15W	<0.0001
D *vs.* D+P 15W	0.0127
P *vs.* D+P 15W	0,0046
IgG *vs.* D 17W	0.8559
IgG *vs.* D+P 17W	0.0165
D *vs.* D+P 17W	0.0052

Fig 3A RT2-PNET	% Survival
IgG *vs.* D	0.0002
IgG *vs.* P	0.1473
IgG *vs.* D+P	<0.0001
D *vs.* D+P	0.0009
P *vs.* D+P	<0.0001

Fig 3A MMTV-PyMT	Day 0	Day 2	Day 5	Day 8	Day 11	Day 14
IgG *vs.* D	0.5584	0.0931	0.0649	0.0022	0.0022	0.0022
IgG *vs.* P	0.6991	0.132	0.0152	0.0043	0.0152	0.0411
IgG *vs.* D+P	0.4848	0.4848	0.0022	0.0022	0.0022	0.0022
D *vs.* D+P	0.1017	0.3939	0.1926	0.132	0.0043	0.0043
P *vs.* D+P	0.2554	0.3939	0.0931	0.0152	0.0022	0.0022

Fig 3B	% $CD11b^+pS6^+$
RT2-PNET	
IgG *vs.* D 15W	0.8203
IgG *vs.* D+P 15W	0.8203
D *vs.* D+P 15W	0.1985
IgG *vs.* D 17W	0.0401
IgG *vs.* D+P 17W	0.5339
D *vs.* D+P 17W	0.0102
MMTV-PyMT	
IgG *vs.* D	0.0424
IgG *vs.* P	0.038
IgG *vs.* D+P	0.0001
D *vs.* D+P	<0.0001
P *vs.* D+P	0.091
NFpp10-GBM	
IgG *vs.* B	0.0083
IgG *vs.* P	0.0492
IgG *vs.* B+P	0.0076
B *vs.* B+P	<0.0001
P *vs.* B+P	<0.0001

Fig 3C	$CD8^+$	GzB^+
RT2-PNET		
IgG *vs.* D 15W	0.0258	0.026
IgG *vs.* P 15W	0.675	0.7771
IgG *vs.* D+P 15W	0.0098	0.0012
D *vs.* D+P 15W	0.8573	0.7308
P *vs.* D+P 15W	0.0082	0.0012
IgG *vs.* D 17W	0.9512	0.2095
IgG *vs.* D+P 17W	0.0105	0.0095
D *vs.* D+P 17W	0.0139	0.0286
MMTV-PyMT		
IgG *vs.* D	0.2075	0.0315
IgG *vs.* P	0.3538	>0.9999
IgG *vs.* D+P	0.0333	<0.0001
D *vs.* D+P	0.002	0.0503
P *vs.* D+P	0.1696	0.0078
NFpp10-GBM		
IgG *vs.* B	0.0653	0.0152
IgG *vs.* P	0.0594	0.9329
IgG *vs.* B+P	0.3046	0.0015
B *vs.* B+P	0.347	0.2136
P *vs.* B+P	0.574	0.07

Fig 3D	% $CC3^+$
RT2-PNET	
IgG *vs*. D 15W	0.004
IgG *vs*. P 15W	0.0366
IgG *vs*. D+P 15W	0.0167
D *vs*. D+P 15W	0.0414
P *vs*. D+P 15W	0.9598
IgG *vs*. D 17W	0.0754
IgG *vs*. D+P 17W	0.0069
D *vs*. D+P 17W	<0.0001
MMTV-PyMT	
IgG *vs*. D	0.1304
IgG *vs*. P	0.5737
IgG *vs*. D+P	0.0002
D *vs*. D+P	0.0011
P *vs*. D+P	0.0011
NFpp10-GBM	
IgG *vs*. B	0.9675
IgG *vs*. P	0.7857
IgG *vs*. B+P	0.8413
B *vs*. B+P	0.7922
P *vs*. B+P	0.5714

Fig 4A	% $CD11c^+$
RT2-PNET	
IgG *vs*. D 15W	0.3312
IgG *vs*. D+P 15W	0.006
D *vs*. D+P 15W	0.0124
IgG *vs*. D 17W	0.3
IgG *vs*. D+P 17W	0.0004
D *vs*. D+P 17W	0.002
MMTV-PyMT	
IgG *vs*. D	0.5468
IgG *vs*. P	0.3689
IgG *vs*. D+P	0.0227
D *vs*. D+P	0.0245
P *vs*. D+P	0.0911
NFpp10-GBM	
IgG *vs*. B	0.9654
IgG *vs*. P	0.5404
IgG *vs*. B+P	0.6941
B *vs*. B+P	0.6913
P *vs*. D+P	0.6160

Fig 4B, C	*Cd40*	*Il10*	*Il12*	*Perforin*
RT2-PNET				
IgG *vs.* D	0.602	0.097	0.004	0.0162
IgG *vs.* P	0.0444	0.004	0.004	0.0465
IgG *vs.* D+P	0.0059	0.0101	0.0147	0.0004
D *vs.* D+P	0.0032	0.0219	0.4799	0.023
P *vs.* D+P	0.5910	0.6419	0.0042	0.0022
MMTV-PyMT				
IgG *vs.* D	0.0162	>0.9999	0.899	0.0004
IgG *vs.* P	0.0015	0.0066	0.0011	0.8749
IgG *vs.* D+P	0.004	0.004	0.004	<0.0001
D *vs.* D+P	0.0002	0.0002	0.0002	<0.0001
P *vs.* D+P	0.3100	0.6103	0.1569	<0.0001
NFpp10-GBM				
IgG *vs.* B	0.198	0.0424	0.004	0.268
IgG *vs.* P	0.004	0.6545	0.0263	<0.0001
IgG *vs.* B+P	>0.9999	0.5374	0.004	<0.0001
B *vs.* B+P	>0.9999	0.1371	0.0165	<0.0001
P *vs.* D+P	0.0019	>0.9999	0.9591	<0.0001

Fig 5A	$CD31^+$ vessels
RT2-PNET	
IgG *vs.* D 15W	<0.0001
IgG *vs.* D+P 15W	<0.0001
D *vs.* D+P 15W	0.3493
IgG *vs.* D 17W	0.0755
IgG *vs.* D+P 17W	<0.0001
D *vs.* D+P 17W	<0.0001
MMTV-PyMT	
IgG *vs.* D	<0.0001
IgG *vs.* P	0.0009
IgG *vs.* D+P	<0.0001
D *vs.* D+P	0.4011
P *vs.* D+P	0.0026
NFpp10-GBM	
IgG *vs.* B	<0.0001
IgG *vs.* P	0.0552
IgG *vs.* B+P	<0.0001
B *vs.* B+P	0.8326
P *vs.* D+P	0.0061

Fig 5B	% $CD31^+NG2^+$ area
RT2-PNET	
IgG *vs.* D 15W	<0.0001
IgG *vs.* D+P 15W	<0.0001
D *vs.* D+P 15W	0.0235
IgG *vs.* D 17W	<0.0001
IgG *vs.* D+P 17W	<0.0001
D *vs.* D+P 17W	0.0024
MMTV-PyMT	
IgG *vs.* D	0.0235
IgG *vs.* D+P	<0.0001
D *vs.* D+P	0.0012
NFpp10-GBM	
IgG *vs.* B	0.9436
IgG *vs.* B+P	0.0128
B *vs.* B+P	0.0408

Fig 5C	% MECA79$^+$CD31$^+$ vessels
RT2-PNET	
IgG *vs.* D	>0.9999
IgG *vs.* P	0.0047
IgG *vs.* D+P	0.0006
D *vs.* D+P	0.0006
P *vs.* D+P	0.0023
MMTV-PyMT	
IgG *vs.* D	0.8048
IgG *vs.* P	0.7104
IgG *vs.* D+P	0.0023
D *vs.* D+P	0.0175
P *vs.* D+P	0.0175
NFpp10-GBM	
IgG *vs.* B	>0.9999
IgG *vs.* P	>0.9999
IgG *vs.* B+P	0.4615
B *vs.* B+P	0.4615
P *vs.* D+P	0.4615

Fig 6A	MMTV-PyMT	RT2-PNET
CD3$^+$	<0.0001	<0.0001
CD8$^+$	<0.0001	<0.0001
CD4$^+$	<0.0001	<0.0001
B220$^+$	<0.0001	<0.0001

Fig 6C	*Ccl19*	*Ccl21*	*Glycam1*	*Cxl13*	*Ccl7*	*Il7*	*Light*
MMTV-PyMT							
IgG *vs.* D	0.0286	0.3429	0.8	0.1333	0.2857	>0.9999	0.2
IgG *vs.* P	0.0286	0.3429	>0.9999	0.6429	0.6857	0.4278	0.3429
IgG *vs.* D+P	0.0286	0.0286	0.1333	0.1333	0.0286	0.0007	0.0286
D *vs.* D+P	0.0286	0.0286	0.2	0.0286	0.0286	0.0002	0.0286
P *vs.* D+P	0.0286	0.0286	0.0095	0.0095	0.0286	<0.0001	0.0286
RT2-PNET							
IgG *vs.* D	0.3429	>0.9999	0.6286	0.0286	0.8857	>0.9999	0.6857
IgG *vs.* P	0.0571	0.6857	0.8	0.4571	0.1143	0.3429	0.4857
IgG *vs.* D+P	0.0286	0.0286	0.0687	0.198	0.0286	0.3429	0.0286
D *vs.* D+P	0.0286	0.0286	0.1091	0.2141	0.0286	>0.9999	0.0286
P *vs.* D+P	0.0286	0.0286	0.1091	0.2141	0.0286	0.2857	0.0286
NFpp10-GBM							
IgG *vs.* B	0.4857	0.0571	0.4286	0.9048	0.2571	0.8857	>0.9999
IgG *vs.* P	0.0286	0.6857	0.4818	0.2788	0.5714	0.3429	0.6857
IgG *vs.* B+P	0.0286	0.0286	>0.9999	0.9048	0.3143	0.8857	0.0286
B *vs.* B+P	0.0286	0.0286	0.5887	0.9372	>0.9999	0.6857	0.0286
P *vs.* B+P	0.2	0.0286	0.607	0.8518	0.6857	0.4857	0.0286

Fig 7B, C, D, E, F	HEV per tumor area	CD8$^+$ per vessel	GzB$^+$CD8$^+$/CD8$^+$	CC3$^+$ area	Necrosis
IgG *vs.* D+P	0.0002	0.0139	<0.0001	<0.0001	0.0635
IgG *vs.* D+P+Ag	0.0062	<0.0001	<0.0001	<0.0001	0.0159
IgG *vs.* D+P+Ant	0.979	<0.0001	<0.0001	0.9926	0.1143
D+P *vs.* D+P+Ag	0.0932	0.0009	0.0039	0.5866	0.0079
D+P *vs.* D+P+Ant	0.0451	0.3589	0.8977	0.0002	0.1905
D+P+Ag *vs.* D+P+Ant	0.0159	0.012	0.0025	<0.0001	0.0159

Fig 7G	Day 0	Day 4	Day 7	Day 10	Day 14	Day 17	Day 21	Day 24	Day 28	Day 30
IgG *vs.* D+P	>0.9999	0.6857	0.1143	0.0286	0.0286	0.0571	0.0286			
IgG *vs.* D+P+Ag	0.6857	0.4857	0.0286	0.0286	0.0571	0.0571	0.0286			
D+P *vs.* D+P+Ag	0.8857	>0.9999	0.3429	0.6857	>0.9999	0.8857	0.8857	0.8857	>0.9999	0.7

Fig 7H	% $MECA79^+CD31^+$ vessels
B+P *vs.* B+P+Ag	0.0008

Fig 7I, J	GzB^+	Tumor burden
IgG *vs.* Ag	0.2	0.7
IgG *vs.* B+P	0.8571	0.8571
IgG *vs.* B+P+Ag	0.0457	0.0571
Ag *vs.* B+P	0.4	0.6286
Ag *vs.* D+P+Ag	0.0571	0.0571
D+P *vs.* D+P+Ag	0.0286	0.0286

fig S3	B20S (50µg/ml)	IFNγ (50 ng/ml)	Hypoxia (1% O_2)
RT2-PNET			
0 *vs.* 4	0.0012	0.0164	0.0286
0 *vs.* 8	0.2614	0.0002	0.1333
0 *vs.* 16	0.3054	0.0002	0.1333
0 *vs.* 24	0.8212	0.0002	0.1333
0 *vs.* 48	0.1186	0.0002	0.0286
MMTV-PyMT			
0 *vs.* 4	0.662	0.0183	0.1508
0 *vs.* 8	0.4857	0.0183	0.254
0 *vs.* 16	0.8589	0.0183	0.0079
0 *vs.* 24	0.7097	0.0007	0.1508
0 *vs.* 48	0.5707	0.0007	0.0079
NFpp10-GBM			
0 *vs.* 4	0.8286	0.0095	0.1508
0 *vs.* 8	0.1457	0.0095	0.6508
0 *vs.* 16	0.6334	0.0095	0.0159
0 *vs.* 24	0.7134	0.0095	0.2222
0 *vs.* 48	0.237	0.0095	0.6905
HcMEC/D3			
0 *vs.* 4	0.3333	0.3333	
0 *vs.* 8	0.6667	0.3333	
0 *vs.* 16	0.6667	0.3333	
0 *vs.* 24	>0.9999	0.3333	
0 *vs.* 48	0.6667	0.3333	
BMDC			
0 *vs.* 4	0.0079	0.0079	0.0317
0 *vs.* 8	0.0079	0.0079	0.0079
0 *vs.* 16	0.0079	0.0079	0.0079
0 *vs.* 24	0.0079	0.0079	0.0079
0 *vs.* 48	0.0079	0.0079	0.0079

fig S4 RT2-PNET	Trial 189	Trial 196
IgG *vs.* D	0.0057	0.0022
IgG *vs.* P	0.3185	0.1536
IgG *vs.* D+P	0.0027	0.0004
D *vs.* D+P	0.0022	0.0119

fig S4 MMTV-PyMT	Day 0	Day 2	Day 5	Day 8	Day 11	Day 14
Trial 168						
IgG *vs.* D	>0.9999	0.2251	0.0043	0.0022	0.0152	0.0087
IgG *vs.* P	0.4848	0.1688	0.0087	0.0649	0.0152	0.026
IgG *vs.* D+P	0.9697	0.6667	0.0022	0.0022	0.0022	0.0022
D *vs.* D+P	0.974	0.4848	0.3095	0.026	0.0043	0.026
P *vs.* D+P	0.2403	0.3095	0.4848	0.1320	0.0260	0.0260
Trial 190						
IgG *vs.* D	0.7302	0.7302	0.1111	0.0159	0.0159	0.0317
IgG *vs.* P	0.4857	0.2	0.0571	0.0286	0.0286	0.0286
IgG *vs.* D+P	0.4127	0.0635	0.0159	0.0159	0.0159	0.0159
D *vs.* D+P	0.5476	0.3095	0.0238	0.0556	0.0317	0.0079
P *vs.* D+P	0.7302	0.7302	0.4127	0.1111	0.1111	0.0635

fig S4 NFpp10-GBM	Trial 148	Trial 156
IgG *vs.* B	0.1993	0.771
IgG *vs.* P	0.5217	0.4152
IgG *vs.* B+P	0.0194	0.103
B *vs.* B+P	0.3968	0.1313
P *vs.* B+P	0.1150	0.0969

fig S5A	*Tnf-α*	*Il12*	*Il23*	*Ccl11*	*Tgf-β*	*Il10*	*Il6*	*Ccl17*
RT2-PNET								
IgG *vs.* D	0.125	0.125	0.0357	0.0357	0.8	0.1333	0.1333	>0.9999
IgG *vs.* P	0.2143	0.2143	0.125	0.2143	>0.9999	0.1333	>0.9999	0.1333
IgG *vs.* D+P	0.0364	0.0364	0.0364	0.0364	0.0444	0.0444	0.0444	0.8889
D *vs.* D+P	0.012	0.0599	0.1119	0.019	0.0081	0.8081	0.004	0.5697
P *vs.* D+P	0.012	0.1898	0.1898	0.019	0.004	0.0162	0.004	0.004
MMTV-PyMT								
IgG *vs.* D	0.3556	0.1798	0.2887	>0.9999	0.8172	0.0999	0.5195	0.022
IgG *vs.* P	0.1798	0.1339	0.5195	0.023	0.1768	0.3576	0.5205	0.0719
IgG *vs.* D+P	0.8142	0.0709	0.013	0.013	0.0709	0.7103	0.7103	0.0719
D *vs.* D+P	0.2886	0.3054	0.0005	0.0003	0.2176	0.2176	0.9705	0.2248
P *vs.* D+P	0.0654	0.7245	0.0003	0.404	0.0068	0.6434	0.9859	0.8126
NFpp10-GBM								
IgG *vs.* B	0.7459	0.0373	0.1215	0.018	0.012	0.2421	0.2601	0.0028
IgG *vs.* P	0.8923	0.305	0.4357	0.537	0.9556	0.9555	0.0441	>0.9999
IgG *vs.* B+P	0.8362	0.2674	0.355	0.6583	0.3553	0.4199	0.2601	0.2601
B *vs.* B+P	0.4359	0.0783	0.0355	0.0524	0.063	0.2101	0.4894	0.2581
P *vs.* B+P	0.776	0.776	0.5169	0.8564	0.2625	0.5774	0.9131	0.2325

fig S5B	IFNγ$^+$ % CD3$^+$CD4$^+$	IFNγ$^+$ % CD3$^+$CD8$^+$
RT2-PNET		
IgG vs. D 15W	0.0022	0.026
IgG *vs.* P 15W	0.0022	0.0043
IgG vs. D+P 15W	0.1014	0.0022
D vs. D+P 15W	0.4452	0.6688
P vs. D+P 15W	0.9452	0.2987
IgG vs. D 17W	0.9048	0.8452
IgG vs. D+P 17W	0.0022	0.0087
D vs. D+P 17W	0.0476	0.0357
MMTV-PyMT		
IgG *vs.* D	0.026	0.0519
IgG *vs.* P	0.366	0.1111
IgG *vs.* D+P	0.0411	0.0043
D *vs.* D+P	0.3939	0.3939
P vs. D+P	0.1375	0.0095
NFpp10-GBM		
IgG *vs.* B	0.6991	0.0262
IgG *vs.* P	0.4848	0.3176
IgG *vs.* B+P	0.9372	0.1282
B *vs.* B+P	0.9372	0.1649
P vs. D+P	0.9372	0.9015

fig S6	*Vegf*	*bFgf*	*Mmp9*	*Il8*	*Cxcl4*	*Cxcl14*	*Cxcl9*	*Cxcl10*
RT2-PNET								
IgG *vs.* D	0.1333	0.2667	0.1333	0.1333	0.1333	0.1333	0.2667	0.1333
IgG *vs.* P	0.8	0.1333	0.1333	0.1333	0.1333	0.1333	0.2667	0.1333
IgG *vs.* D+P	0.0444	0.8889	0.4	>0.9999	0.0444	0.0444	0.1778	0.0444
D *vs.* D+P	0.004	>0.9999	0.5697	0.004	0.3677	0.2141	0.5697	0.004
P *vs.* D+P	0.004	0.0162	0.2828	0.2141	0.0081	0.4606	0.6	0.2141
MMTV-PyMT								
IgG *vs.* D	0.0091	0.4818	0.7105	0.4818	0.8636	0.2818	0.0091	0.4818
IgG *vs.* P	0.0182	0.0091	0.3301	0.2818	0.0091	0.6	0.0091	0.0091
IgG *vs.* D+P	0.0091	0.0091	0.5035	0.0091	0.0091	0.1	0.0091	0.0091
D *vs.* D+P	0.0014	0.1135	0.8167	0.0005	0.0003	0.8633	0.1903	0.0005
P *vs.* D+P	0.1615	0.0003	0.5457	0.0005	0.9314	0.9314	0.6665	0.4363
NFpp10-GBM								
IgG *vs.* B	0.0336	0.3301	0.9399	0.6042	0.6042	0.0503	0.1063	0.0196
IgG *vs.* P	0.0036	0.0005	0.0036	0.0093	0.0366	0.2621	0.0366	0.001
IgG *vs.* B+P	0.3483	>0.9999	0.414	0.0336	0.9399	0.9399	0.3301	0.0056
B *vs.* B+P	0.0625	0.077	0.1359	0.0188	0.9314	0.6048	0.2581	0.3401
P *vs.* B+P	0.0007	<0.0001	0.0027	0.7259	0.0732	0.482	0.0297	0.8038

fig S7A	Copies *Ltβrl* 100 copies *Gapdh*
β-TC3 (RT2-PNET) *vs.* MMTV-PyMT	0.3333
β-TC3 (RT2-PNET) *vs.* NFpp10-GBM	0.3333
MMTV-PyMT *vs.* NFpp10-GBM	0.6667

fig S7B	Cell death	Proliferation
β-TC3 (RT2-PNET)		
0 *vs.* 100 ng/ml Ag	0.2944	0.0411
0 *vs.* 300 ng/ml Ag	0.7619	0.0411
0 *vs.* 100 ng/ml Ant	0.9654	0.2403
0 *vs.* 300 ng/ml Ant	0.9113	0.8182
MMTV-PyMT		
0 *vs.* 100 ng/ml Ag	0.4567	0.9372
0 *vs.* 300 ng/ml Ag	0.513	0.5887
0 *vs.* 100 ng/ml Ant	0.3766	0.9372
0 *vs.* 300 ng/ml Ant	0.4221	0.9372
NFpp10-GBM		
0 *vs.* 100 ng/ml Ag	0.1905	0.0043
0 *vs.* 300 ng/ml Ag	0.0563	0.0022
0 *vs.* 100 ng/ml Ant	0.1558	0.6991
0 *vs.* 300 ng/ml Ant	0.7143	0.3095

fig S8A, B, C, F, G	Tumor burden	HEV per tumor area	CD8+ per vessel	CD3+ per HEV	CD8+ per HEV
IgG *vs.* D+P	0.329	0.1667	0.1128	0.5368	0.1429
IgG *vs.* D+P+Ag	0.5368	0.1429	<0.0001	0.2468	>0.9999
IgG *vs.* D+P+Ant	0.2468	>0.9999	0.5532	0.5476	0.1825
D+P *vs.* D+P+Ag	0.5476	0.1825	0.0213	>0.9999	0.5532
D+P *vs.* D+P+Ant	0.8413	0.2857	0.4418	0.1825	0.0213
D+P+Ag *vs.* D+P+Ant	0.8413	0.1429	0.0008	0.0213	0.0286

fig S8D	RT2-PNET HEV per tumor area	MMTV-PyMT HEV per tumor area
IgG *vs.* D+P	0.1667	0.0002
IgG *vs.* D+P+Ag	0.1429	0.0062
IgG *vs.* D+P+Ant	>0.9999	0.979
IgG *vs.* Ag	0.0286	0.9333
IgG *vs.* Ant	>0.9999	0.2
D+P *vs.* D+P+Ag	0.1825	0.0932
D+P *vs.* D+P+Ant	0.2857	0.0451
D+P *vs.* Ag	0.2321	0.0444
D+P *vs.* Ant	0.2857	0.0444
D+P+Ag *vs.* D+P+Ant	0.1429	0.0159
D+P+Ag *vs.* Ag	0.4	0.1905
D+P+Ant *vs.* Ant	>0.9999	0.2381